Journal of Cleaner Production 338 (2022) 130678

Contents lists available at ScienceDirect

Journal of Cleaner Production

journal homepage: www.elsevier.com/locate/jclepro

Characterization of rheological properties and aging performance of bitumen modified by bio-oil from bamboo charcoal production

Haotong Lin [a,1], Qi Chen [b,1], Xue Luo [b], Yuqing Zhang [c], Kai Miao [a], Tan Li [a], Kaige Wang [a,*]

[a] State Key Laboratory of Clean Energy Utilization, Zhejiang University, Hangzhou, 310027, China
[b] College of Civil Engineering and Architecture, Zhejiang University, Hangzhou, 310058, China
[c] Department of Civil Engineering, Aston University, Birmingham, B4 7ET, UK

ARTICLE INFO

Handling Editor: Zhen Leng

Keywords:
Bio-bitumen
Slow pyrolysis
Bio-oil
Rheological properties
Aging performance

ABSTRACT

As a waste stream from charcoal production, the liquid bio-oil has not been properly used, leading to both environmental and economic issues. In this study, this deleterious waste was explored as a promising additive for petroleum-based bitumen. Raw bio-oil was pretreated through distillation under different temperature to remove undesirable components. The resulting medium and heavy bio-oil fractions were blended with petroleum-based bitumen by weight ratios up to 12% to obtain bio-bitumen. The rheological and aging properties of the bio-bitumen were further evaluated with various test means. The results showed that the addition of bio-oil had softening effect on bitumen. Bio-bitumen performed better brittleness resistance with smaller Glover-Rowe parameters and better fatigue crack resistance at shorter crack length than that of base bitumen. The lower non-recoverable creep compliance of the heavy fraction modified bio-bitumen indicated its better rutting resistance, compared to that of the base bitumen. Characterization of the carbonyl and sulfoxide functional groups in the aged bitumen showed comparative aging performance of the bio-bitumen modified with heavy fraction. The findings of this study indicate that the promising potential of bio-oil heavy fraction to replace petroleum-based bitumen for generating sustainable road paving material.

1. Introduction

Bitumen, the residual fraction from crude oil after naphtha, gasoline, kerosene and other fractions were extracted, is used as a binder in asphalt concrete for road paving. (Yang and Suciptan, 2016). According to Asphalt Institute and Eurobitume, the current world production of bitumen is approximately 87 Million tonnes per year (Asphalt Institute, Eurobitume, 2015). However, with the improvement of petroleum refining technology, production of bitumen has decreased. Moreover, there is an increasing demand for a sustainable and environment friendly material to replace the petroleum-derived bitumen to reduce the greenhouse gas emission (Schwartz, 1993).

Both academia and industry are making a continuing effort to explore a renewable material that can meet the performance requirements of road construction (Gao et al., 2020; Wang et al., 2021; Wu et al., 2009). Among these explored materials, bio-oil obtained from thermochemical processes of biomass either pyrolysis and hydrothermal has gained increasing interests to serve as a binder in the road construction (Ding et al., 2021; Fini et al., 2011; Lv et al., 2020; Raouf and Williams, 2011; Shao et al., 2021; Wang et al., 2020). Bio-oil or bio-crude derived from biomass feedstock including agricultural and forestry wastes and animal excreta is typically a viscous liquid with black or dark brown color (Mohan et al., 2006; Xiu and Shahbazi, 2012). Bio-oil shared certain similarity with bitumen in physicochemical properties like similar solubility characteristics and high viscosity (Fini et al., 2011; Mullen and Boateng, 2008). Replacing bitumen partially or totally with bio-oil results in a new pavement material, which is uniformly named as bio-bitumen or bio-binder (Raouf and Williams, 2009; Yang et al., 2018).

The previous studies mainly focused on the performance evaluation on bio-bitumen (Fini et al., 2015; Gao et al., 2018b; Hosseinnezhad et al., 2015). Fini et al. (2012) investigated the performance of swine manure-based bitumen (blended with 2, 5, 10 wt% bio-oil, respectively). They concluded that bio-oil can reduce the viscosity, complex modulus, rutting depth, cracking temperature (1.4 °C, 3.0 °C, 4.6 °C, respectively) and aging characteristics, compared to the base bitumen. Raouf and

* Corresponding author.
E-mail address: kaigewang@zju.edu.cn (K. Wang).
[1] These authors contributed equally to this work and should be considered co-first authors.

https://doi.org/10.1016/j.jclepro.2022.130678
Received 10 October 2021; Received in revised form 12 January 2022; Accepted 23 January 2022
Available online 25 January 2022

Williams (2011) employed pyrolysis bio-oils from switchgrass and oakwood to make bio-bitumen at the ratio of 25 wt%. The bio-bitumen was found to have slightly lower high and intermediate temperature performance grades in comparison to the unmodified bitumen. While the low temperature performance grades were lost by about 10 °C after the addition of the bio-oil. Yang and You (2015) verified the high-temperature performance of 5% and 10% original bio-oil (with 15–30 wt% water) and de-watered bio-oil (with 5–8 wt% water) modified bitumen was 23.7%, 29.8%, 28.5% and 55.9% higher than that of the base bitumen, respectively. Ingrassia et al. (2019) and Raouf and Williams (2009) claimed that bio-binders had similar or even better aging resistance as compared to conventional bitumen with similar penetration grade. Wang's research studied the performance of bio-bitumen with various addition ratios and verified the positive effect of bio-oil on cracking resistance. Unaged and RTFO-aged bio-bitumen with 5% bio-oil could meet the requirements resulted from the penetration, softening point, ductility and other indexes and the temperature sensitivity of bio-bitumen with 5% bio-oil was the smallest (Gao et al., 2018a; Wang et al., 2020; Zhang et al., 2017).

Due to the complexity of the bio-oil, bio-bitumen in some circumstance might be failed to satisfy the performance requirements of pavement bitumen materials. Bio-bitumen with high substitution ratio of bio-oil (30% and 70% by weight) was found that the light molecular components of bio-oil volatilized and lost during the aging process, and the chemical bonds were more susceptible to be attacked by oxygen, which accelerated the oxidation of bio-bitumen (Yang et al., 2015, 2017). Williams' study suggests that the bio-oil could not be used as a direct alternative binder in the pavement industry due to the presence of water (about 10 wt%) and high volatiles (Raouf and Williams, 2009). It has investigated that bitumen modified by bio-oil (5 wt% and 10 wt%) generated from waste wood resources damaged the low-temperature performance, which resulted from the critical low-temperature of 5 wt % and 10 wt% original bio-oil and de-watered bio-oil (with about 5% moisture) modified bitumen were 0.63 °C, 3.33 °C, 3.58 °C and 4.73 °C higher than that of the base bitumen, respectively (Yang et al., 2013, 2014). Sun et al. (2016) studied the bio-bitumen modified with 0, 2, 4, 6 and 8% bio-oil which contained 3.1% moisture and found that the high temperature performance was inhibited.

Meanwhile, bio-oil obtained from slow pyrolysis charcoal production as co-product, although its yield is about 35 wt%, has not been properly and efficiently utilized (Al Arni, 2018). The bio-oil is difficult to be applied as advanced fuel, due to its poor physical and chemical properties, such as high water content and strong acidity (Stamatov et al., 2006; Xiu and Shahbazi, 2012). A large amount of slow pyrolysis oil has been wasted, resulting in serious environmental pollution. Therefore, in view of the existing problems in the previous research of bitumen this study proposed a strategy of utilizing the bio-oil from charcoal production. We hypothesis that the bio-oil after removing the moisture and light volatiles can be conducive to make the bio-bitumen performance similar to or even better than that of petroleum-based bitumen. In this study, bio-oil pretreatment method was developed. The influence of different pretreatment parameters, and dosage of bio-oil on the properties of bio-bitumen were evaluated in this study with focus on its rheological properties and aging behavior.

2. Materials and methods

2.1. Materials

The base bitumen used in this study was a 70-penetration grade bitumen (denoted by 70#) that was supplied from Hebei Transportation Investment Group Corporation. The basic properties (penetration, softening point, and ductility) of 70# bitumen was shown in Table 1. It can be seen that the basic properties of the bitumen meet the requirements of the specification (MOTO, 2011). Raw bio-oil was obtained from a charcoal production plant at Fujian province of China. The bio-oil was a by-product derived from bamboo through slow pyrolysis, which was a dark brown and viscous liquid as shown in Fig. 1(a). The moisture content of the raw bio-oil was 11.52 wt% by a volumetric Karl Fischer titrator (V10S, America METTLER TOLEDO). The viscosity of the raw bio-oil was 43.13 cP (@ 60 °C) by a viscometer (LVDV-II + P, America Brookfield).

Table 1
Basic properties of 70# bitumen.

Properties	Unit	Requirement	Result	Method
Penetration	0.1 mm	60–80	66.2	T0604-2011(MOTO, 2011)
Softening point	°C	≥46	49.0	T0606-2011(MOTO, 2011)
Ductility at 5 °C	cm	≥20	38	T0605-2011(MOTO, 2011)

2.2. Methods

2.2.1. Pretreatment of bio-oil

In this experiment, two fractions acquired from the pretreatment of raw bio-oil were used to obtain bio-bitumen. One fraction with moisture content of 1–2 wt% was obtained by heating the raw bio-oil from room temperature to 130 °C through the atmospheric distillation to remove most of the water and some light components. The resulting liquid named as bio-oil A is a medium fraction. Heavy fraction, namely bio-oil B, was the heavy distillate with the boiling point above 300 °C from the raw bio-oil. In this distillation process to obtain bio-oil B, raw bio-oil was firstly heated from room temperature to 110 °C at atmospheric pressure for dehydration, and then heated up from 110 °C to 300 °C under a pressure of 7–12 mmHg to remove most of the light components. A rotary belt distillation system (36–100, America B/R Instrument) was applied for the pretreatment of raw bio-oil. The heat rate was set to 20% during the distillation.

As shown in Fig. 1(b) and (c), bio-oil A maintained the flow state with poor fluidity and bio-oil B has become solid at room temperature. Physicochemical properties of the base bitumen and bio-oils studied were summarized in Table 2. The element contents of raw bio-oil were quite different from that of base bitumen, which was manifested in lower carbon content (64.24% vs. 81.85%). After distillation, the elemental composition of the two bio-oil fractions was closer to that of base bitumen, especially bio-oil B. Gradually the moisture content decreased with the distillation process, which was conducive to the production of bio-bitumen. The viscosity and density of the bio-oils increased by distilling. However, the molecular weight of bio-oils before and after distillation was significantly lower than that of base bitumen.

The chemical compositions of the two bio-oil fractions were analyzed by an Agilent Gas Chromatography-Mass Spectrometry (GC-MS) (a 5977B Mass Spectrometry coupled with a 7890B Gas Chromatograph). The result is summarized as shown in Table 3. Bio-oil A was mainly composed of phenols, esters, furans, ketones, alkanes and benzenes, with phenols accounting for the majority. After further distillation, the volatile substances in bio-oil B, such as furans, ketones and benzenes, were cut only 3.97% phenols were retained. Alkanes (21.8%) and esters (56.23%) were the dominant compounds in Bio-oil.

2.2.2. Preparation of bio-bitumen

The 70# bitumen without any additives was investigated as the base bitumen in this study. Bio-oil A and B was added to the 70# bitumen at the weight ratio of 6% and 12%. Thus, a total of five types of bitumen was investigated: 70# bitumen, and the 6 wt% bio-oil A (A6), 12 wt% bio-oil A (A12), 6 wt% bio-oil B (B6), 12 wt% bio-oil B (B12) modified bitumen, as given in Table 4. The base bitumen was firstly heated to 135 °C. The bio-oils were preheated at 150 °C before being

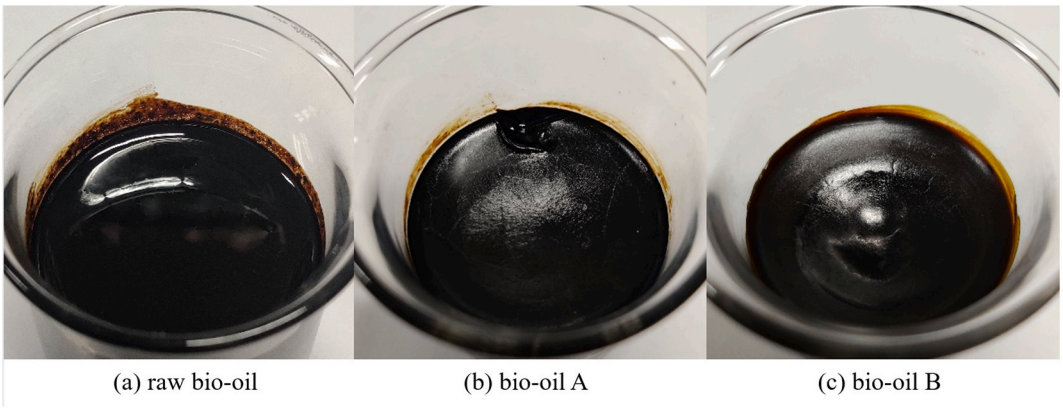

Fig. 1. Physical appearance of the raw bio-oil and the two fractions after pretreatment.

Table 2
Typical physicochemical properties of base bitumen and bio-oils used in this study.

Properties		Base bitumen	Raw Bio-oil	Bio-oil A	Bio-oil B
Carbon (wt%)		81.85	64.24	68.64	76.69
Hydrogen (wt%)		9.55	7.25	7.33	9.26
Nitrogen (wt%)		0.56	0.33	0.47	0.39
Oxygen (wt%)		-[b]	28.18[a]	23.56[a]	13.66[a]
Moisture (wt%)		-[c]	11.52	1.42	-[c]
Viscosity @ 60 °C (cP)		-[b]	43.13	89.77	236.19
Density (g/cm^{-1})		-[b]	1.05	1.08	1.16
Molecular weight	M_n	808	264	216	254
	M_w	1786	425	440	430
	D	2.21	1.61	2.03	1.69

[a] Oxygen content was calculated by subtraction.
[b] Not analyzed.
[c] Below detection limitation.

homogeneously mixed with 70# bitumen at 150 °C for 20 min in a high-speed shear mixer with a rotational speed of 1500 rpm. During the blending process, extra attentions were taken to avoid excessive heating temperature and time, which may lead to accelerated bio-bitumen aging.

2.2.3. Aging simulation of bio-bitumen

In order to evaluate the aging performance of bio-bitumen, it is necessary to simulate aging of bitumen during the service life. Based on the standard test specified in AASHTO R28 (AASHTO, 2009), the bio-bitumen investigated in this study were exposed in the Pressure Aging Vessel (PAV) (9500, America Prentex) under the aging condition of 2.1 MPa air pressure and 100 °C for 5 h, 10 h, 20 h, 40 h and 60 h, respectively. On the basis of the previous research, 5 h PAV was used instead of RTFO/TFOT to simulate the short-term aging of bitumen, which is of great significance for the research of bitumen aging in different terms to reduce the influence of variables from different aging simulation method (Migliori and Corté, 1998; Sun et al., 2014; Tian et al., 2021).

2.2.4. Rheological testing

The rheological properties of bitumen were tested by Dynamic Shear Rheometer (DSR) (DHR-2, America TA Instruments). The standard procedure of DSR test followed AASHTO T315 (AASHTO, 2010).

2.2.4.1. Frequency sweep. The frequency sweep test was to determine the viscoelastic property of bitumen in a broad range of temperatures and frequencies. The experiment was conducted from 0.01 Hz to 100 Hz at seven test temperatures, ranging from 10 °C to 70 °C with an increment of 10 °C. During the test, the strain values of the bitumen samples were controlled at 0.2% for 10 °C–30 °C and 0.5% for 40 °C–70 °C respectively to ensure that the material response was within the linear viscoelastic region. According to the specification requirements, the 25 mm diameter parallel plates with a 1 mm testing gap was applied to the test condition above 40 °C, and an 8 mm diameter parallel plates with a 2 mm testing gap was used at the temperature below 30 °C (AASHTO, 2010). The test samples were the PAV-5 h aged and PAV-20 h aged bitumen.

In accordance with the time-temperature superposition principle (TTSP), when a test temperature condition is difficult to achieve in practice, a suitable temperature can be taken as a reference temperature, and the frequency at other temperatures can be transformed into the reduced frequency at the reference temperature (Yusoff et al., 2011). Therefore, the dynamic shear modulus and phase angle at other temperatures can be equivalent to those of the reduced frequency at the reference temperature, respectively. The time-temperature equivalent factor equation used in this study was Williams-Landel-Ferry (WLF) equation (Williams et al., 1955):

$$\lg\alpha_T = \frac{-C_1(T - T_0)}{C_2 + T - T_0} \tag{1}$$

$$\omega_r = \alpha_T \times \omega \tag{2}$$

where α_T is the time-temperature equivalent factor; C_1 and C_2 are the fit parameters; T and T_0 are the actual test temperature and the reference temperature, respectively; ω_r and ω are the actual test angular frequency and reduced angular frequency, respectively.

Based on the TTSP, there are some models commonly used to describe the master curve of bitumen, such as The Sigmoidal Model, the Generalized Logistic Sigmoidal Model, the Christensen-Anderson (CA) Model and the Christensen-Anderson-Marasteanu (CAM) Model (Asgharzadeh et al., 2015; Yusoff et al., 2013). CAM model have an outstanding correlation between the measured and fitted data for the modified bitumen than other models (CholewiŃSka et al., 2018; Yusoff et al., 2013). The viscoelastic performance of bitumen can be studied from the master curves of complex shear modulus and phase angle at an expanded range of temperatures and frequencies. The CAM model can be shown as follows (Olard and Di Benedetto, 2011; Yusoff et al., 2011):

$$|G^*| = \frac{G_g^*}{\left[1 + \left(\frac{\omega_c}{\omega_r}\right)^v\right]^{\frac{w}{v}}} \tag{3}$$

$$\delta = \frac{90w}{1 + \left(\frac{\omega_r}{\omega_c}\right)^v} \tag{4}$$

where $|G^*|$ is the complex shear modulus; G_g^* is the glassy shear modulus;

Table 3
Chemical compounds of the two bio-oil fractions.

Chemical compounds	Relative content (peak area/%)		Formula
	Bio-oil A	Bio-oil B	
Furans	**5.46**	**–**	
Ethanone, 1-(2-furanyl)-	2.92	–	$C_6H_6O_2$
Furan-2-carbonyl chloride, tetrahydro-	2.54	–	$C_5H_7ClO_2$
Ketones	**5.18**	**–**	
3-Cyclopentene-1-acetaldehyde	0.60	–	$C_7H_8O_2$
2-oxo-; 2-Cyclopenten-1-one, 2-methyl-	0.43	–	C_6H_8O
2-Cyclopenten-1-one, 2,3-dimethyl-	1.89	–	$C_7H_{10}O$
2-Ethyl-3-methylcyclopent-2-en-1-one	2.25	–	$C_8H_{12}O$
Phenols	**64.45**	**3.97**	
Phenol	7.99	–	C_6H_6O
Phenol, 2-ethyl-5-methyl-	0.82	–	$C_9H_{12}O$
Phenol, 2-methoxy-	5.27	–	$C_7H_8O_2$
Phenol, 2-methyl-	2.94	–	C_7H_8O
Phenol, 3-methyl-	6.03	–	C_7H_8O
Phenol, 2-methoxy-3-methyl-	0.50	–	$C_8H_{10}O_2$
Creosol	6.24	–	$C_8H_{10}O_2$
Phenol, 3-ethyl-5-methyl-	0.38	–	$C_9H_{12}O$
Phenol, 4-ethyl-	9.56	–	$C_8H_{10}O$
Phenol, 3,4-dimethyl-	2.36	–	$C_8H_{10}O$
Phenol, 4-ethyl-2-methoxy-	4.59	–	$C_9H_{10}O_2$
Phenol, 3-(1-methylethyl)-	0.55	–	$C_9H_{12}O$
Phenol, 2,3,5-trimethyl-	0.30	–	$C_9H_{12}O$
Phenol, 3-ethyl-5-methyl-	1.26	–	$C_9H_{12}O$
Phenol, 4-propyl-	1.17	–	$C_9H_{12}O$
Phenol, 2-methoxy-4-propyl-	1.78	–	$C_{10}H_{14}O_2$
Phenol, 2,6-dimethoxy-	8.06	–	$C_8H_{10}O_3$
Phenol, 2-methoxy-5-(1-propenyl)-, (E)-	0.97	–	$C_{10}H_{12}O_2$
5-tert-Butylpyrogallol	2.19	–	$C_{10}H_{14}O_3$
Phenol, 2,6-dimethoxy-4-(2-propenyl)-	0.86	–	$C_{11}H_{14}O_3$
Guaiacol, 4-butyl-	–	1.05	$C_{11}H_{16}O_2$
(E)-2,6-Dimethoxy-4-(prop-1-en-1-yl) phenol	–	2.91	$C_{11}H_{14}O_3$
Alkanes	**2.21**	**21.80**	
Ethylene oxide	0.32	0.91	C_2H_4O
17-Pentatriacontene	1.89	5.31	$C_{35}H_{70}$
Heptacosane	–	15.59	$C_{27}H_{56}$
Benzenes	**2.94**	**–**	
3,4-Dimethoxytoluene	0.28	–	$C_9H_{12}O_2$
3,5-Dimethoxy-4-hydroxytoluene	2.66	–	$C_9H_{12}O_3$
Esters	**11.13**	**56.23**	
Octadecanoic acid, 4-hydroxy-, methyl ester	1.66	–	$C_{19}H_{38}O_3$
Pentadecanoic acid, 13-methyl-, methyl ester	1.82	–	$C_{17}H_{34}O_2$
Dasycarpidan-1-methanol, acetate (ester)	7.65	25.19	$C_{20}H_{26}N_2O_2$
Propanoic acid, 2-methyl-, (dodecahydro-6a-hydroxy-9a-methyl-3-methylene-2,9-dioxoazuleno[4,5-b] furan-6-yl) methyl ester, [3aS-(3aα,6β,6aα,9aβ,9bα)]-	–	2.72	$C_{19}H_{26}O_6$
Hexadecanoic acid, methyl ester	–	4.62	$C_{17}H_{34}O_2$
Ethyl iso-allocholate	–	2.37	$C_{26}H_{44}O_5$
10-Octadecenoic acid, methyl ester	–	9.48	$C_{19}H_{36}O_2$
Hexadecanoic acid, 14-methyl-, methyl ester	–	2.73	$C_{18}H_{36}O_2$
Hexadecanoic acid, 16-methyl-, methyl ester	–	4.27	$C_{19}H_{38}O_2$
Cholestan-3-one, cyclic 1,2-ethanediyl aetal, (5β)-	–	1.98	$C_{29}H_{50}O_2$
Butanoic acid, 1a,2,5,5a,6,9,10,10a-octahydro-5,5a-dihydroxy-4-(hydroxymethyl)-1,1,7,9-tetramethyl-11-oxo-1H-2,8a-methanocyclopenta[a]cyclopropa[e]cyclodecen-6-yl ester, [1aR-(1aα,2α,5β,5aβ,6β,8aα,9α,10aα)]-	–	2.87	$C_{24}H_{34}O_6$

Table 4
Summary of tested bitumen.

Types	Name	Proportion		
		Bio-oil A	Bio-oil B	Base bitumen
Base bitumen	70#	–	–	100 wt%
Bio-bitumen	A6	6 wt%	–	94 wt%
	A12	12 wt%	–	88 wt%
	B6	–	6 wt%	94 wt%
	B12	–	12 wt%	88 wt%

ω_c is the crossover angle frequency; ω_r is the reduced angular frequency; v and w are the fit parameters of master curve model; δ is the phase angle.

2.2.4.2. Time sweep. Fatigue is generally a concern at intermediate temperatures (10 °C–30 °C). Under the rotational shear load, the crack of bitumen expands from the outer edge to the center, leading to the degradation of bitumen fatigue performance (Zhang and Gao, 2019). Recently, a crack growth model based on damage mechanics has been reported, which can accurately predict the crack length of bitumen under different shear fatigue loading and material conditions (Hintz and Bahia, 2013; Li et al., 2021; Zhang and Gao, 2019). The fatigue crack length can be calculated by the formula as follows (Zhang and Gao, 2019):

$$CL = \left\{1 - \left[\frac{|G_N^*|/\sin(\delta_N)}{|G_0^*|/\sin(\delta_0)}\right]^{1/4}\right\} r_0 \quad (5)$$

where CL is the fatigue crack length of the bitumen at the N^{th} load cycle; $|G_0^*|$ and δ_0 are the complex shear modulus and phase angle of the bitumen in the undamaged state, respectively; $|G_N^*|$ and δ_N are the complex shear modulus and phase angle of the bitumen at the N^{th} load cycle in the damaged state, respectively; r_0 is the original radius of the sample (i.e., 4 mm in this study).

The evaluation of fatigue is normally evaluated for bitumen after long-term aging (PAV 20 h), as they were stiffer and thus more prone to crack (Ameri et al., 2018; Ingrassia et al., 2020). Therefore, the PAV-20 h aged bitumen was tested at 20 °C and 10 Hz for 40 min under the controlled strain loading mode. To receive reliable test results for the bitumen during the time loading process, the strain level was controlled as 5% (Shan et al., 2017; Wang et al., 2015, 2016).

2.2.4.3. Multiple stress creep and recovery (MSCR). With regard to the high temperature performance of bitumen, many studies have focused on the rutting index ($|G^*|/\sin\delta$) from the DSR test (Gao et al., 2018b; Raouf et al., 2010; Sun et al., 2016). Previous research has concluded that non-recoverable creep compliance (J_{nr}) and the percent recovery (R) in MSCR test have been more reliable in correlation with pavement rutting performance of bio-bitumen (D'Angelo, 2011; Harman et al., 2011; Yang and You, 2015; Zhang et al., 2016).

Therefore, the MSCR test was performed on the DSR to characterize the high temperature performance of bitumen in this study (D7405-15, 2015). The bitumen underwent PAV 5 h aging was applied and the testing temperature was 64 °C. In MSCR test, the first ten creep (1s) and recovery (9s) cycles were carried out under a shear load of 0.1 kPa. Then a shear load of 3.2 kPa was applied to the same sample for another 10 cycles. There were totally 20 cycles. As mentioned, J_{nr} is the rutting index in the MSCR test (Li et al., 2019; Sun et al., 2019). The expressions of J_{nr} are as follows:

$$J_{nr}(\tau, N) = \left(\gamma_r^N - \gamma_0^N\right)/\tau \quad (6)$$

$$J_{nr}(\tau) = \frac{1}{10}\sum_{N=1}^{10} J_{nr}(\tau, N) \quad (7)$$

where τ is the applied shear stress of 0.1 kPa and 3.2 kPa, respectively; γ_0^N is the initial creep strain value for each cycle; γ_r^N is the final strain value in the recovery stage for each cycle; N = 1, 2, 3, …, 10 is the loading cycle number for each stress level.

2.2.5. Fourier transform infrared (FTIR) spectroscopy

FTIR can analyze the molecular structure and identify the compounds of substances according to the relative vibration and rotation of molecules (Van den Bergh, 2011; Yang et al., 2015). The FTIR equipment used was Germany Bruker vertex 70 in this experiment. The test

samples were prepared by dissolving fully the bitumen in tetrahydrofuran (THF) solvent with a concentration of 80 mg/mL, followed by dropping 15 μL of each sample solution onto the potassium bromide (KBr) tablet with a pipette gun. The FTIR test was carried out on the formed sample film after the complete evaporation of the solvent. The FTIR test parameters were wavelength range 4000 cm^{-1}–400 cm^{-1}, resolution 4 cm^{-1}, and scan number 16 times. In order to compare the aging degree of bio-bitumen at different aging terms, multiple aging times were considered, i.e., unaged, PAV-5 h, PAV-10 h, PAV-20 h, PAV-40 h and PAV-60 h.

According to Lambert-Beer's law, the test results are affected by sample concentration and film thickness in FTIR. Although the concentration of the samples has been controlled, the absorption spectrums were still normalized in order to alleviate those influence (Lamontagne et al., 2001).

It has researched that the oxidation of bitumen can be characterized by the change of specific infrared absorption peaks of carbonyl and sulfoxide functional groups (Ge et al., 2019; Nie et al., 2020). In order to reduce the effect of sample amount on the results in a way, the carbonyl index (*CI*) and sulfoxide index (*SI*) were utilized to determine quantitatively the aging behavior of bitumen defined as below:

$$CI = \frac{A_{1700}}{A_{1375} + A_{1459}} \tag{8}$$

$$SI = \frac{A_{1030}}{A_{1375} + A_{1459}} \tag{9}$$

$$\Delta CI = CI_i - CI_0 \tag{10}$$

$$\Delta SI = SI_i - SI_0 \tag{11}$$

where A_{1700} is the carbonyl area (≈1700 cm^{-1}); A_{1459} and A_{1375} are the reference areas; A_{1030} is the sulfoxide area (≈1030 cm^{-1}); CI_0 and SI_0 are the *CI* and *SI* of unaged bitumen, respectively; CI_i and SI_i are the *CI* and *SI* of aged bitumen, respectively; $i = 5, 10, 20, 40, 60$, the aging time for bitumen.

The absorption peak area was calculated by the integral intensity method. The tangent line of the lowest points on both sides of the absorption peak was taken as the baseline and the area covered by the absorption peak was directly measured.

The detailed experimental procedures were illustrated in Table 5.

3. Results and discussions

3.1. Rheological properties analysis

3.1.1. Black diagram

The principal viscoelastic parameters obtained from the DSR test are the magnitude of the complex shear modulus (G*) and the phase angle (δ). G* is defined as the ratio of maximum shear stress to maximum strain, which provides a measure of the total resistance of the bitumen to deformation under shear load (Airey, 2002). δ is the phase or time lag between the stress and strain applied during the test, and it is defined as the ratio of the elastic and viscous components (Gao et al., 2018b). The black diagram expressed the functional relationship between G* (on logarithmic scale) and δ (on normal scale). Since the influence of the frequency and temperature parameters are eliminated during the analysis process, all data can be displayed in the graph without the need to perform the TTSP on the original data (Airey, 2002). Generally, black diagram is used to evaluate the viscoelastic properties of bitumen, including modified bitumen (Ingrassia et al., 2020).

Fig. 2(a) and (b) presented the relationship between G* and δ of five bitumen after PAV 5 h and 20 h aging, respectively. It can be observed that the experimental data of different bitumen aligned along the same curve, which indicated that they exhibited a thermo-rheologically simple behavior, thus allowing the master curves of the rheological properties to be obtained (Airey, 2002). At each aging condition, compared with the base bitumen, the black diagram curve shifted to lower G* and δ with the content of bio-oil A increased, which showed that bio-oil A degraded the stiffness of bio-bitumen and improved its elastic behavior. The δ of A6 and A12 was significantly different from that of 70# at a low level of G^* (below 10 kPa) under the condition of PAV-5 h aged as summarized in Fig. 2(a), reflecting the difference of viscoelastic behavior between them and 70#. While this phenomenon was alleviated after a longer aging time, as shown in Fig. 2(b), it may be due to the volatilization loss of lighter molecules in the bio-oil A added to A6 and A12 during this period. Instead, the viscoelastic behavior of B6 and B12 was more similar to that of 70#, whether PAV 5 h or 20 h aged, as their data fitted tightly together in the black diagram.

3.1.2. Master curve

Based on the thermo-rheologically simple behavior of bitumen evidenced by the black diagram, the master curves of bitumen were fitted by the nonlinear least square using the CAM model mentioned above according to the TTSP (Rowe et al., 2007). In the master curve, the three-dimensional characterization of complex modulus (or phase angle), time and temperature were simplified to two-dimensional format (complex modulus or phase angle, reduced frequency) and dynamic mechanical data were plotted against reduced frequency on a log-log scale (or semi-log) (Anderson et al., 1994; Marateanu and Anderson, 1996). 20 °C was selected as the reference temperature of the master curves in this test. The fitting parameters and correlation coefficients of the master curves of complex modulus and phase angle were shown in Tables S1 and S2 in the Appendix, respectively. It can be seen from the tables that the overall fitting effect was excellent.

Fig. 3 provided the complex modulus master curves of the bitumen under two aging time. In the case of each bitumen, the overall trend was that the G^* increased with the reduced frequency. It was found from Fig. 3(a) that addition of bio-oils had an effect of mollification and reduce the stiffness as evidenced by the lower G* of all bio-bitumen, and this effect enhanced with the increase content of the same bio-oil. The value of G* was arranged in descending order of 70#, B6, B12, A6 and A12 and bio-oil A occupied the optimal position. The G* of A6 and A12 were significantly lower than that of 70#, which was consistent with the result of black diagram.

Compared with the aging condition of PAV-5 h, the softening effect of bio-bitumen was weakened after 20 h PAV aging, as proved by the vertical shift of G* plotted in Fig. 3(b). Although the G* of A6 and A12 has increased, it was still below 70#. On the contrary, the G* of B6 and B12 gradually approached that of 70# and the curve of B12 almost coincided with that of 70#. From the displacement of each bitumen curve in Fig. 3(a) and (b), the stiffening effect caused by aging on bio-oil A modified bitumen was more remarkable than others.

The phase angle master curves of the bitumen were plotted in Fig. 4. In the low frequency (high temperature) area of Fig. 4(a) and Fig. S2(a)

Table 5
Experimental procedures.

Test method	Purpose	Test parameters	bitumen tested
PAV	Short and long term aging	100 °C, 2.1 MPa, 5 h, 10 h, 20 h, 40 h, and 60 h	Unaged
Frequency sweep	Stiffness	70, 60, 50 and 40 °C, 10 Hz, 0.5% strain \ 30, 20, and 10 °C, 10 Hz, 0.2% strain	PAV-5 h and PAV-20 h aged
Time sweep	Fatigue	20 °C, 10 Hz, 5% strain, for 40 min	PAV-20 h aged
MSCR	Rutting	64 °C	PAV-5 h aged
FTIR	Aging evaluation	Room temperature	Unaged, PAV-5 h, PAV-10 h, PAV-20 h, PAV-40 h and PAV-60 h aged

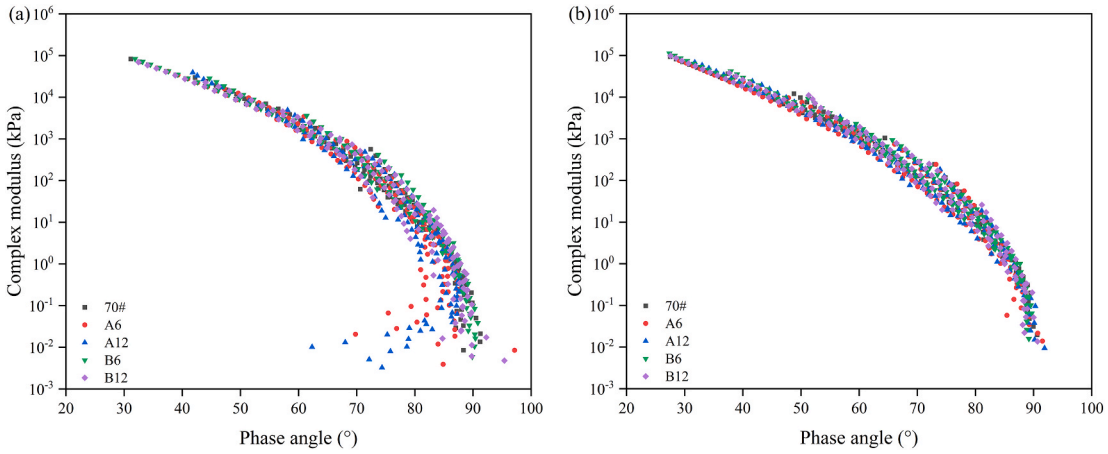

Fig. 2. Black diagram of different bitumen (a) PAV-5 h aged; (b) PAV-20 h aged.

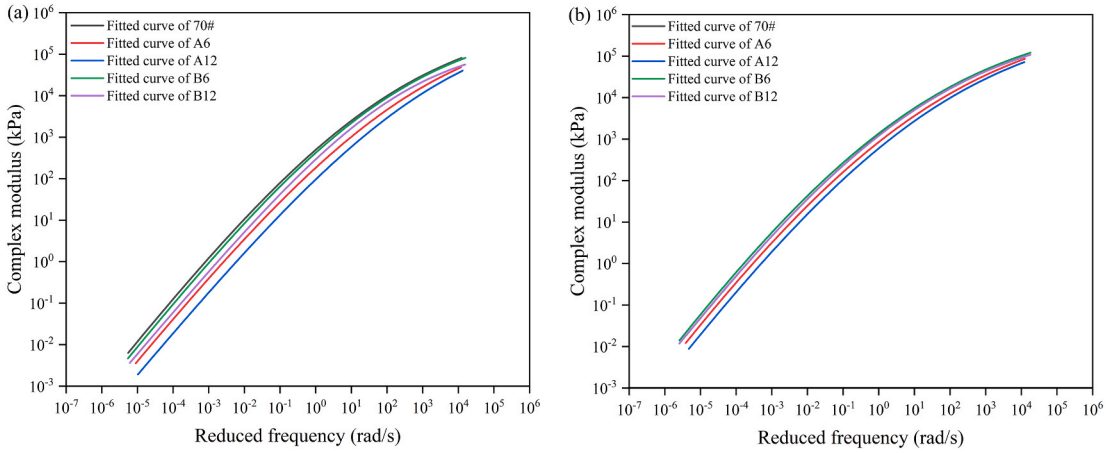

Fig. 3. Master curve of complex modulus for bitumen (a) PAV-5 h aged; (b) PAV-20 h aged.

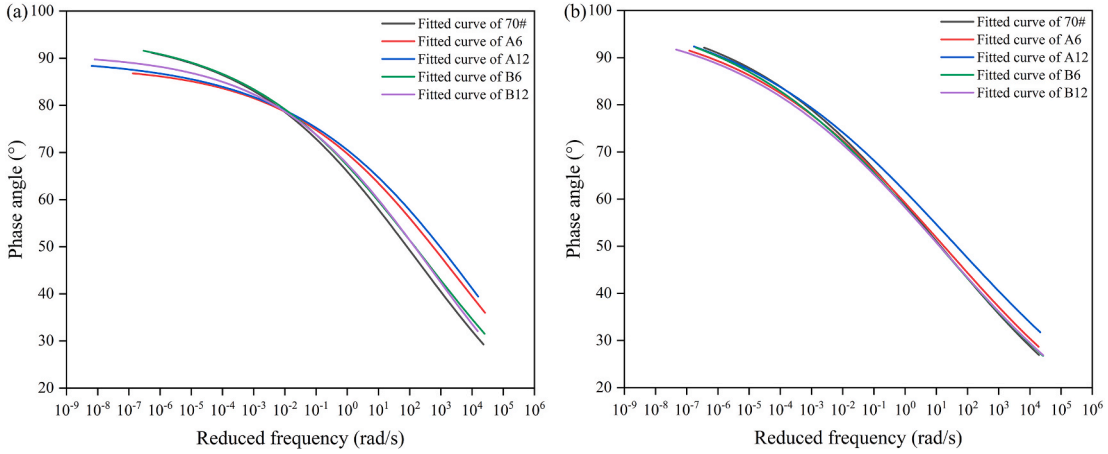

Fig. 4. Master curve of phase angle for bitumen (a) PAV-5 h aged; (b) PAV-20 h aged.

in the Appendix, the data points of A6 and A12 scattered completely and the fitted curve did not show a nice correlation with the measured data, which demonstrated that A6 and A12 were difficult to showed regular rheological behavior under the applied strain load. In contrast, the rheological behavior of bio-bitumen modified with bio-oil B basically remained unchanged. The δ of B6 and B12 was sequentially lower than 70# in the low frequency (high temperature) area, indicating that bio-oil B made the bitumen more elastic than viscous, which meant B6 and B12 were able to restore their original shape after load deformation. Nevertheless, bio-bitumen had better viscosity related to the low temperature performance with the higher δ of all bio-bitumen than 70# in the high frequency (low temperature) section.

Comparing Fig. 4(a) and (b), the increased aging time did not significantly change the trend of phase angle of bio-bitumen in the high frequency (low temperature) region. However, it can be seen from Fig. 4 (b) and Fig. S2(b) in the Appendix that the δ of PAV-20 h aged bio-bitumen fitted well in the low frequency (high temperature) region, which was different from PAV-5 h aged bitumen in Fig. 4(a) and Fig. S2 (a). Considering the two different aging times, the increased phase angle indicated the viscosity grew in the low frequency region and phase angle decreased meant the elasticity increased in the high frequency area, which represented that the high-temperature performance and low-temperature performance were both impaired after longer aging term.

3.1.3. Glover-Rowe parameter

The evaluation of bitumen embrittlement and block cracking potential was mainly worked out by testing the ductility or cracking temperature from the Bending Beam Rheometer (BBR) test in previous reports (Lu and Isacsson, 2001; Marek, 1977; Ruan et al., 2003; You et al., 2011). Recently, it has been found that the Glover-Rowe (*G-R*) parameters received from the master curve have been used as prospective indicators of bitumen cracking resistance, which is of greatly importance to the convenience of bitumen laboratory testing (Glover et al., 2005; Hajj et al., 2016; Mensching et al., 2015; Rowe, 2011; Ruan et al., 2003; Zhang et al., 2020). The expression was summarized as follows (Anderson et al., 2011; King et al., 2012):

$$G-R = \frac{|G^*|\cos^2\delta}{\sin\delta} \tag{12}$$

where $|G_0^*|$ is the complex shear modulus and δ is the phase angle.

The *G-R* parameters captured the $|G_0^*|$ and δ at 15 °C and 0.005 rad/s of the master curves, which was determined from the frequency sweep test data fitted at the reference temperature of 15 °C (Glover et al., 2005; Rowe, 2011). A low *G-R* value is desired for the brittleness resistance of bitumen (Cao et al., 2019). The *G-R* parameters of PAV 5 h and 20 h aged bitumen and the increment rate of them emerged in Fig. 5.

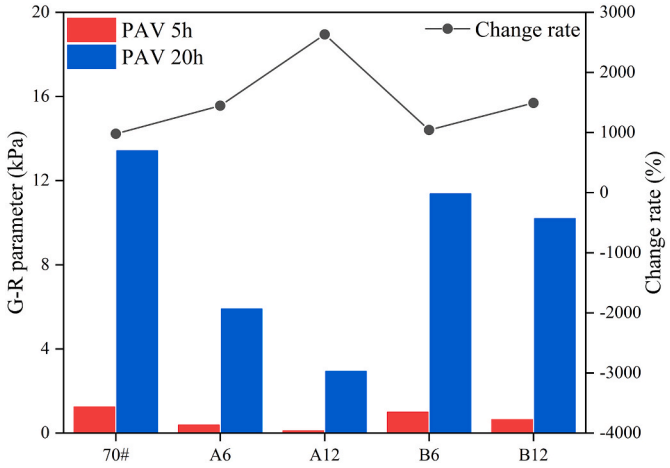

Fig. 5. *G-R* parameter of bitumen.

It can be recognized that addition of bio-oils made the bio-bitumen *G-R* values lower than base bitumen under 5 h and 20 h PAV-aging terms, which meant an improved low-temperature brittleness resistance of bio-bitumen. The *G-R* values of A6, A12, B6, B12 were 69.31%, 91.36%, 20.07%, 48.54% under PAV-5 h aging and 55.99%, 78.11%, 15.23%, 24.03% under PAV-20 h aging lower than that of 70#, respectively. Furthermore, the improvement of bio-oil A was more significant than that of bio-oil B, and for the same bio-oil fraction, the *G-R* value decreased with the increase of dosage, which was beneficial to replace petroleum bitumen with bio-oil. Normally, a longer aging term hardened and embrittled the bitumen material and considerably impaired its fragile resistance, which was reflected in the rapid growth of *G-R* with higher aging levels. Bio-oil A modified bitumen represented a higher aging sensitivity in terms of the change rate of *G-R*, and the better performer in this regard was B6 close to that of 70#.

3.1.4. Fatigue crack length

Crack typically occurs inside the bitumen or at the bitumen-aggregate interface. Thus, the fatigue resistance of bitumen plays a critical role in overall pavement performance (Hintz and Bahia, 2013).

Fig. 6 presented fatigue crack length of the five bitumen for PAV-20 h aged and showed that the crack length rose over the span of the number of load cycles. Based on the fracture mechanics of viscoelasticity, the crack length curves of the bitumen can be divided into three stages: the initiation period (Stage I), transition period (Stage II) and propagation period (Stage III) (Li et al., 2021). In Stage I, the crack length grew sharply with an increase in the number of cycles, and it stayed almost constant in Stage II. In Stage III, the crack length increased at an almost linear rate.

It can be obtained from Fig. 6 that bio-oils substantially reduced the fatigue crack length and strengthened the fatigue crack resistance of bitumen. For each type of bio-bitumen, the fatigue crack length increased with the addition of bio-oil. For the same bio-oil content, at the initial stage of fatigue strain loading, the fatigue crack length of bio-bitumen modified with bio-oil B was lower than that of bio-oil A modified bio-bitumen, but the trend was reversed with the loading time. This was due to that the existence of more light molecules in bio-oil A, which postponed the growth of crack in Stage II and finally shortened the crack length. In general, the two bio-oil fractions were beneficial to fatigue crack resistance of bio-bitumen, as the *CL* of A6, A12, B6, B12 were 23.96%, 33.33%, 13.54%, 27.60% lower than that of 70#, respectively.

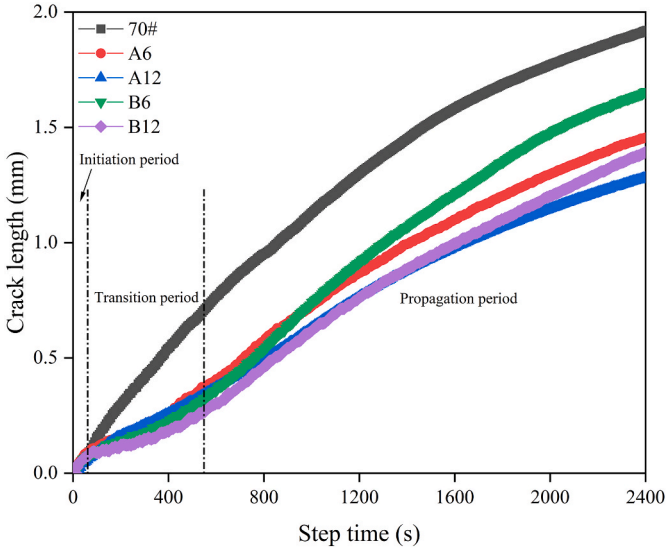

Fig. 6. Crack length of the bitumen for PAV-20 h aged.

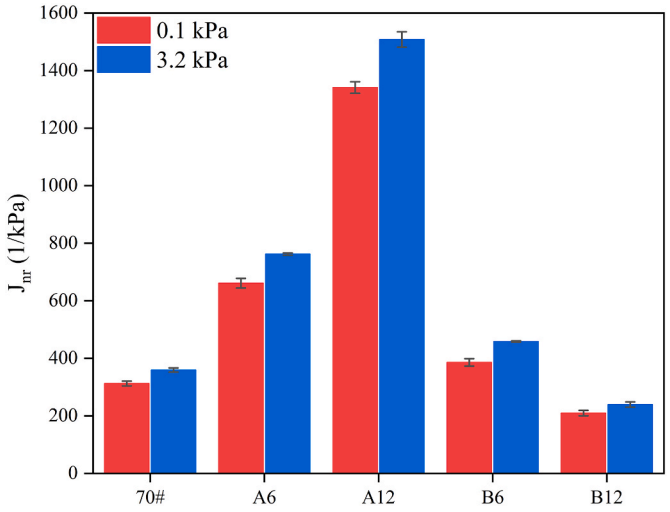

Fig. 7. J_{nr} of PAV-5 h aged bitumen at 0.1 kPa and 3.2 kPa.

3.1.5. The non-recoverable creep compliance

To value the resistance of bio-bitumen against rutting at high temperature, MSCR test was carried out at 64 °C. Typically the higher J_{nr} value, the larger permanent deformation under the repeated load (Yang and You, 2015).

As can be seen from Fig. 7, it was reasonable that the J_{nr} increased with the rise of the stress level for each bitumen. Under the two test stress levels, the J_{nr} of A6 and A12 was far more than that of 70# twice and four times, respectively, which proved A6 and A12 had suffered larger permanent deformation. Instead, the J_{nr} of B6 and B12 were close to that of 70# and decreased as the content of bio-oil B increased. Among them, B12 had the best anti-rutting performance with the lowest J_{nr}. According to ASTM D7405 and AASHTO MP 19 (D7405-15 A, 2015; MP19, 2010), J_{nr} at 3.2 kPa predominantly characterizes the rutting resistance of bitumen. Consequently, B12 had better rutting resistance (i.e., high temperature performance) than that of 70# and it was accepted that the rutting resistance of B6 was slightly inferior than 70#.

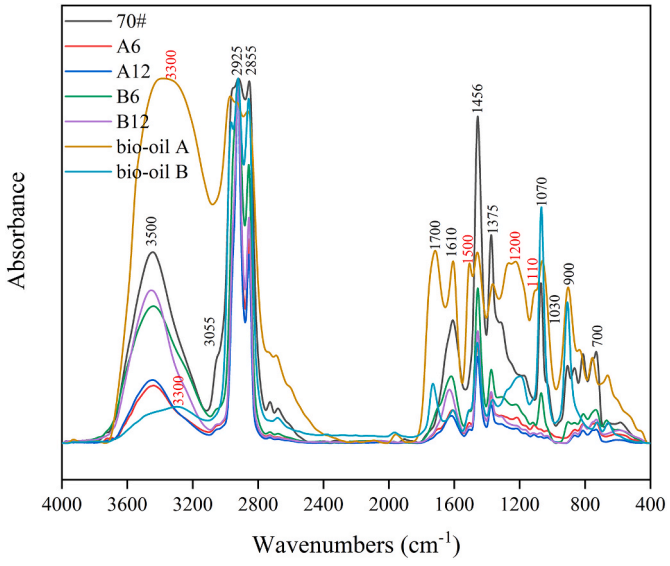

Fig. 8. FTIR spectra of different bitumen in unaged condition and the two fractions of bio-oil.

3.2. FTIR analysis

3.2.1. Functional groups

The variations of peak height and band areas of some certain bonds in FTIR spectrum have been widely applied to qualitatively and quantitatively analyze the oxidation of bitumen (Fini et al., 2016; Petersen, 2009). Adopting band areas more instead of the peak height for two reasons: (1) the variations of band areas are less (Yut and Zofka, 2011), and (2) it's difficult to obtain the single peak height resulting from vibrations may occur in the same band (Lamontagne et al., 2001).

It was observed from Fig. 8 that the main peaks for the five types of bitumen and two fractions of bio-oil were located at 3055 cm^{-1} (C—H stretch), 2925 and 2855 cm^{-1} (CH_2 stretch), 1700 cm^{-1} (C═O stretch), 1610 cm^{-1} (C═C stretch), 1456 cm^{-1} (CH_2 bend), 1375 cm^{-1} (CH_3 bend), 1030 cm^{-1} (S═O stretch) and 900 to 700 cm^{-1} (C—H bend). For the bio-bitumen and two fractions of bio-oil, there were additional peaks at 1500 cm^{-1} (C═C stretch) and 1110 cm^{-1} (C—O stretch). The peaks of 3300 cm^{-1} (O—H stretch of phenolic hydroxyl) and 1200 cm^{-1} (C—OH stretch) for the aromatics appeared in the bio-oils. Besides, there was a peak at 3450 cm^{-1} (O—H stretch) that mainly derived from (1) the moisture in the air was absorbed in the KBr tablets and samples during the test, and (2) hydroxyl groups on phenols and benzenes from the samples. The absorption peak at 1070 cm^{-1} resulted from the incomplete volatilization of the solvent (THF) used. Fig. 8 illustrated that the spectrograms of several bio-bitumen were almost consistent with the base bitumen and there were no additional peaks, indicating that there is a great possibility that no chemical reaction between bio-oils and bitumen.

3.2.2. Carbonyl and sulfoxide aging behavior

Due to the oxidation of certain types of carbon and sulfur compounds after aging, the sulfoxide (S═O) and carbonyl (C═O) absorption peaks appear at 1030 cm^{-1} and 1700 cm^{-1} for the bitumen, respectively (Ge et al., 2019; Nie et al., 2020). As shown in Fig. 9, the longer aging time, the greater intensity of those absorption peaks, so they can be used as the main objects of quantitative analysis to reflect the aging degree of the bitumen (Ouyang et al., 2006; Petersen, 2009; Xu and Huang, 2010).

Fig. 10 and Fig. 11 reflected the trend of the *CI* and *SI* increments of the aged bitumen and the unaged bitumen with aging time. It can be observed form Fig. 10 that for each bitumen, the overall trend of the ΔCI arose with the increase of aging time, which indicated that the aggravation of bitumen aging degree. For different types of bio-bitumen, under the same aging time, the ΔCI of A12 was significantly higher than that of 70#, which may result from more aromatic components and oxygen content of bio-oil A. Further, the existence of C═C stretch and C—O stretch in bio-oil A, as Fig. 8 shown, made bitumen more vulnerable to been attacked by oxygen, which contributed to the formation of carbonyl functional groups. On the contrary, B12 possessed the anti-oxidation effect, and its ΔCI was lower than that of 70# in aging time of 10 h, 20 h and 40 h. B6 also presented a near aging degree to the base bitumen, in terms of the near ΔCI values.

The calculation results of ΔSI were exhibited in Fig. 11. On the whole, the tendence was similar to ΔCI. In terms of ΔCI and ΔSI, A6 also showed the close aging level to the base bitumen with aging time, indicating that the relatively small amount of bio-oil A had little effect on the aging of bitumen compared to A12. The ΔSI of B6 and B12 were usually lower than that of 70#. For the reason, bio-oil B may prevent the formation of S═O during the aging, but this effect diminished as the content of bio-oil B increased. Overall, B6 and B12 had better anti-aging performance than A12. This conclusion was consistent with the rheological properties analyzed above.

4. Summary and conclusions

Bio-bitumen obtained from blending base bitumen with a certain percentage (6 wt% and 12 wt%) of pretreated bio-oil was investigated

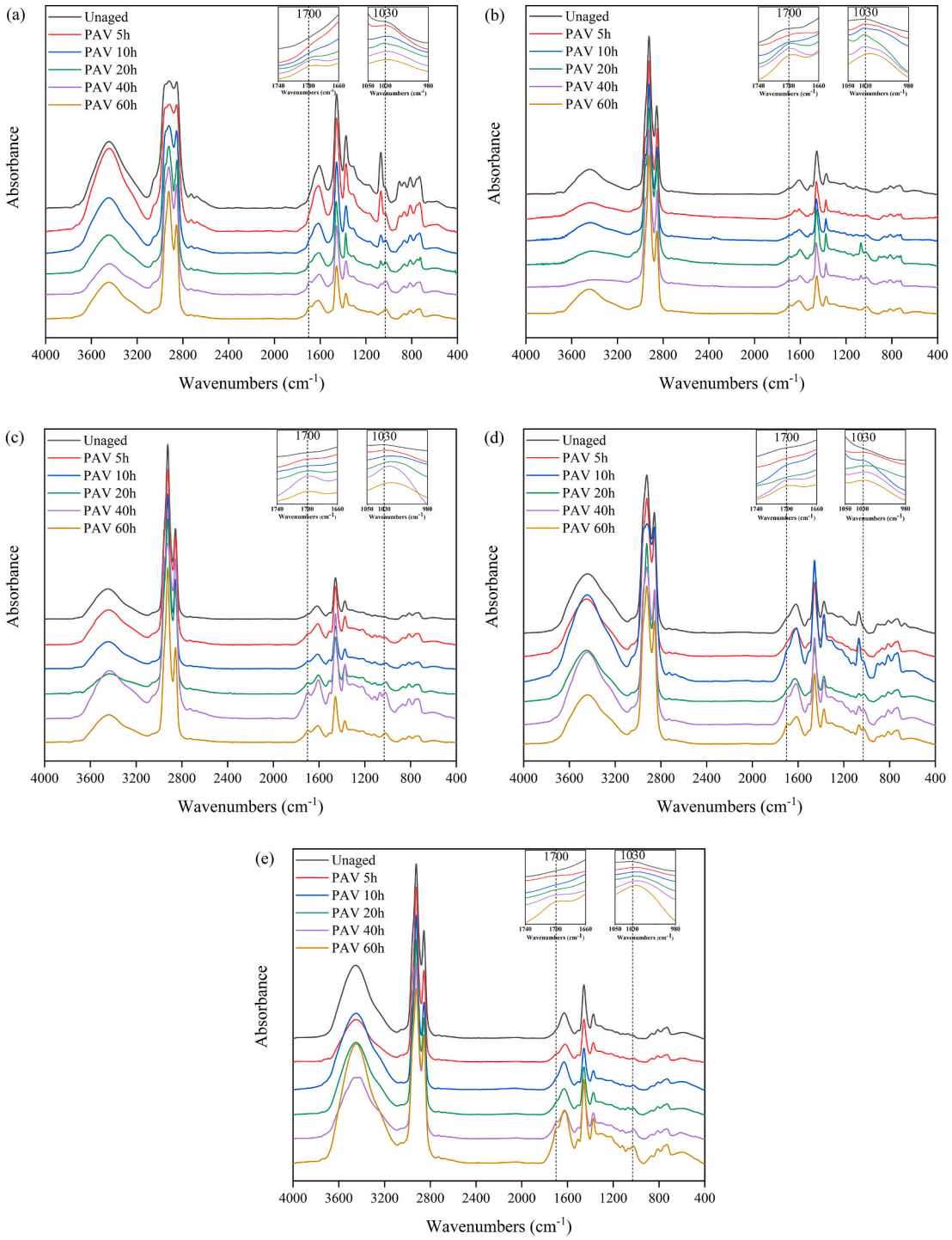

Fig. 9. FTIR spectra of different bitumen under different aging time (a) 70#; (b) A6; (c) A12; (d) B6; (e) B12.

with focus on its rheological properties and aging performance. Bio-oil A with moisture content of 1–2 wt% is a medium fraction, which was obtained by heating the raw bio-oil from room temperature to 130 °C through the atmospheric distillation. Bio-oil B removed the components with the boiling point below above 300 °C is the heavy fraction obtained by atmospheric and vacuum distillation. Through various aging times simulation (PAV 5 h, 10 h, 20 h, 40 h, 60 h), the rheological properties and aging performance of bitumen were fully analyzed by the test of frequency sweep, time sweep, MSCR and FTIR. The conclusions of this present study can be drawn as follows:

(1) Based on their similar thermo-rheological simple behavior, the complex modulus master curves indicated that bio-oils had softening effect under the same aging time, and the effect enhanced with the dosage of the same bio-oil, which was beneficial for compaction and workability of bitumen. Longer aging time performed a greater stiffening impact on bio-oil A modified bitumen. In addition, from the phase angle master curves, bio-bitumen showed more viscous that was desired for low temperature performance as shown in the high frequency region. B6 and B12 with higher elasticity in the low frequency region represented the

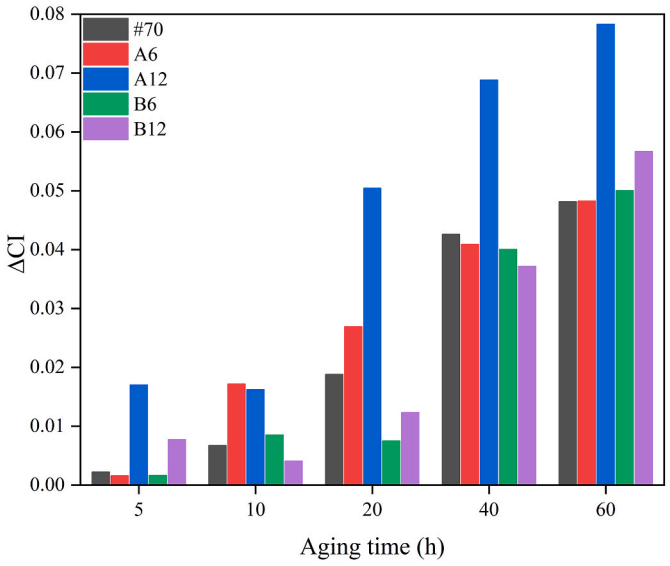

Fig. 10. *ΔCI* of bitumen at different aging time.

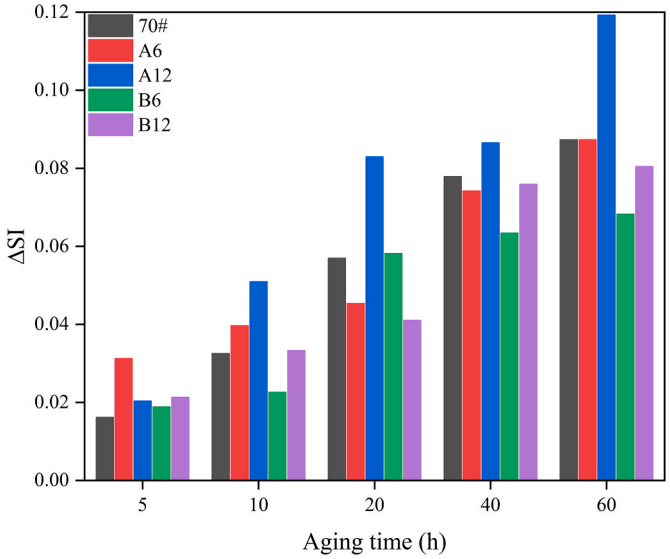

Fig. 11. *ΔSI* of bitumen at different aging time.

improved high temperature rutting resistance. While these two performances were both impaired after longer aging term.

(2) The *G-R* parameters obtained from the master curve at 15 °C reference temperature confirmed that bio-bitumen with lower *G-R* values provided better embrittlement resistance. Although the improvement of bio-oil A modified bitumen was the best, their aging sensitivity was also the most obvious.

(3) According to the fatigue test based on damage mechanics, increased dosage of bio-oil in modification usually represented improved fatigue resistance at shorter crack length. After longer load cycles, the fatigue crack degree of bio-oil A modified bitumen was smaller because of its more significant softening effect evidenced by the master curves analysis.

(4) The addition of bio-oil B improved the deformation resistance and elastic recovery performance of base bitumen and B12 came out at the head of the list, but bio-oil A performed a negative effect, given by the MSCR test for evaluating high temperature rutting performance.

(5) Compared of FTIR spectra, bio-oils and bio-bitumen existed additional functional groups of C═C stretch and C—O stretch. Besides, there is possibility no chemical reaction between bio-oils and base bitumen for no other absorption peaks of bio-bitumen. The *ΔCI* and *ΔSI* showed that the addition of bio-oil A accelerated the aging degree. The oxidation of bio-oil B modified bitumen had not changed much in the case of *ΔCI*, while bio-oil B may prevent the formation of S═O during aging and the effect diminished with the increase of its content. The anti-aging performance of B6 and B12 was within acceptable range, which may be desirable for the long-term application of bitumen.

The results shown in this study suggests that the bio-oil B after water and light components removed can be used as a potential binder for replacing petroleum bitumen to produce sustainable bio-bitumen material. The findings of this study also provide a promising utilization method for the waste stream from charcoal production. However, further studies need to be conducted to evaluate the low temperature anti-cracking, the moisture-resistance performance on the bitumen modified with bio-oil B, and whether the bio-bitumen can still meet the requirements (such as storage stability) by adding a higher dosage of bio-oil B.

CRediT authorship contribution statement

Haotong Lin: Investigation, Data curation, Formal analysis, Writing – original draft. **Qi Chen:** Investigation, Data curation, Formal analysis. **Xue Luo:** Writing – review & editing. **Yuqing Zhang:** Methodology, Writing – review & editing. **Kai Miao:** Investigation. **Tan Li:** Investigation. **Kaige Wang:** Conceptualization, Supervision, Writing – review & editing, All authors have checked the manuscript and have agreed to the submission.

Declaration of competing interest

The authors declare that they have no known competing financial interests or personal relationships that could have appeared to influence the work reported in this paper.

Acknowledgements

The authors would like to acknowledge financial support from the National Natural Science Foundation of China (Grant No.: 51906215) and the Fundamental Research Funds for the Central Universities.

Appendix A. Supplementary data

Supplementary data to this article can be found online at https://doi.org/10.1016/j.jclepro.2022.130678.

References

AASHTO, 2009. Standard practice for accelerated aging of asphalt binder using a pressurized aging vessel (PAV). In: American Association of State Highway Transportation Officials.

AASHTO, 2010. Determining the rheological properties of asphalt binder using a dynamic shear rheometer (DSR). In: American Association of State Highway and Transportation Officials.

Airey, G.D., 2002. Use of black diagrams to identify inconsistencies in rheological data. Road Mater. Pavement Des. 3 (4), 403–424. https://doi.org/10.1080/14680629.2002.9689933.

Al Arni, S., 2018. Comparison of slow and fast pyrolysis for converting biomass into fuel. Renew. Energy 124, 197–201. https://doi.org/10.1016/j.renene.2017.04.060.

Ameri, M., Mansourkhaki, A., Daryaee, D., 2018. Evaluation of fatigue behavior of high reclaimed asphalt binder mixes modified with rejuvenator and softer bitumen. Construct. Build. Mater. 191, 702–712. https://doi.org/10.1016/j.conbuildmat.2018.09.182.

Anderson, D.A., Christensen, D.W., Bahia, H.U., Dongre, R., Sharma, M., Antle, C.E., et al., 1994. Binder Characterization and Evaluation, Volume 3: Physical

Characterization. Strategic Highway Research Program, National Research Council, Washington, DC.
Anderson, R.M., King, G.N., Hanson, D.I., Blankenship, P.B., 2011. Evaluation of the relationship between asphalt binder properties and non-load related cracking. J. Assoc. Asphalt Paving Technol. 80.
Asgharzadeh, S.M., Tabatabaee, N., Naderi, K., Partl, M.N., 2015. Evaluation of rheological master curve models for bituminous binders. Mater. Struct. 48 (1), 393–406. https://doi.org/10.1617/s11527-013-0191-5.
Cao, W., Wang, Y., Wang, C., 2019. Fatigue characterization of bio-modified asphalt binders under various laboratory aging conditions. Construct. Build. Mater. 208, 686–696. https://doi.org/10.1016/j.conbuildmat.2019.03.069.
CholewiŃska, M., IwaŃSki, M., Mazurek, G., 2018. The impact of ageing on the bitumen stiffness modulus using the cam model. Baltic J. Road Bridge Eng. 13 (1), 34–39. https://doi.org/10.3846/bjrbe.2018.386.
D'Angelo, J.A., 2011. The relationship of the MSCR test to rutting. Road Mater. Pavement Des. 10 (1), 61–80. https://doi.org/10.1080/14680629.2009.9690236.
D7405-15, A, 2015. Standard test method for multiple stress creep and recovery (MSCR) of asphalt binder using a dynamic shear rheometer. In: USA: Annual Book of ASTM Standards.
Ding, Y., Shan, B., Cao, X., Liu, Y., Huang, M., Tang, B., 2021. Development of bio oil and bio asphalt by hydrothermal liquefaction using lignocellulose. J. Clean. Prod. 288 https://doi.org/10.1016/j.jclepro.2020.125586.
Asphalt Institute, Eurobitume, 2015. The Bitumen Industry, third ed.
Fini, E.H., Kalberer, E.W., Shahbazi, A., Basti, M., You, Z., Ozer, H., et al., 2011. Chemical characterization of biobinder from swine manure: sustainable modifier for asphalt binder. J. Mater. Civ. Eng. 23 (11), 1506–1513. https://doi.org/10.1061/(asce)mt.1943-5533.0000237.
Fini, E.H., Al-Qadi, I.L., You, Z., Zada, B., Mills-Beale, J., 2012. Partial replacement of asphalt binder with bio-binder: characterisation and modification. Int. J. Pavement Eng. 13 (6), 515–522. https://doi.org/10.1080/10298436.2011.596937.
Fini, E.H., Oldham, D., Buabeng, F.S., Nezhad, S.H., 2015. Investigating the aging susceptibility of bio-modified asphalts. Airfield and Highw. Pavements. https://doi.org/10.1061/9780784479216.007.
Fini, E.H., Hosseinnezhad, S., Oldham, D.J., Chailleux, E., Gaudefroy, V., 2016. Source dependency of rheological and surface characteristics of bio-modified asphalts. Road Mater. Pavement Des. 18 (2), 408–424. https://doi.org/10.1080/14680629.2016.1163281.
Gao, J., Wang, H., You, Z., Mohd Hasan, M., Lei, Y., Irfan, M., 2018a. Rheological behavior and sensitivity of wood-derived bio-oil modified asphalt binders. Appl. Sci. 8 (6) https://doi.org/10.3390/app8060919.
Gao, J., Wang, H., You, Z., Mohd Hasan, M.R., 2018b. Research on properties of bio-asphalt binders based on time and frequency sweep test. Construct. Build. Mater. 160, 786–793. https://doi.org/10.1016/j.conbuildmat.2018.01.048.
Gao, J., Wang, H., Liu, C., Ge, D., You, Z., Yu, M., 2020. High-temperature rheological behavior and fatigue performance of lignin modified asphalt binder. Construct. Build. Mater. 230 https://doi.org/10.1016/j.conbuildmat.2019.117063.
Ge, D., Chen, S., You, Z., Yang, X., Yao, H., Ye, M., et al., 2019. Correlation of DSR results and FTIR's carbonyl and sulfoxide indexes: effect of aging temperature on asphalt rheology. J. Mater. Civ. Eng. 31 (7) https://doi.org/10.1061/(asce)mt.1943-5533.0002781.
Glover, C.J., Davison, R.R., Domke, C.H., Ruan, Y., Juristyarini, P., Knorr, D.B., et al., 2005. Development of a New Method for Assessing Asphalt Binder Durability with Field Validation. Texas Dept Transport, pp. 1–334, 1872.
Hajj, E.Y., Morian, N., Sebaaly, P.E., Nabizadeh, H., Pournoman, S., 2016. Evaluation of Adaptive Glover-Rowe Parameter on Aging of Select Modified Binders. Paper presented at the Proc., 95th Annual Meeting of the Transportation Research Board.
Harman, T., Youtcheff, J., Bukowski, J., 2011. The Multiple Stress Creep Recovery (MSCR) Procedure.
Hintz, C., Bahia, H., 2013. Understanding mechanisms leading to asphalt binder fatigue in the dynamic shear rheometer. Road Mater. Pavement Des. 14 (2), 231–251. https://doi.org/10.1080/14680629.2013.818818.
Hosseinnezhad, S., Fini, E.H., Sharma, B.K., Basti, M., Kunwar, B., 2015. Physiochemical characterization of synthetic bio-oils produced from bio-mass: a sustainable source for construction bio-adhesives. RSC Adv. 5 (92), 75519–75527. https://doi.org/10.1039/c5ra10267g.
Ingrassia, L.P., Lu, X., Ferrotti, G., Canestrari, F., 2019. Chemical and rheological investigation on the short- and long-term aging properties of bio-binders for road pavements. Construct. Build. Mater. 217, 518–529. https://doi.org/10.1016/j.conbuildmat.2019.05.103.
Ingrassia, L.P., Lu, X., Ferrotti, G., Canestrari, F., 2020. Chemical, morphological and rheological characterization of bitumen partially replaced with wood bio-oil: towards more sustainable materials in road pavements. J. Traffic Transport. Eng. 7 (2), 192–204. https://doi.org/10.1016/j.jtte.2019.04.003.
King, G., Anderson, M., Hanson, D., Blankenship, P., 2012. Using Black Space Diagrams to Predict Age-Induced Cracking. Paper presented at the 7th RILEM international conference on cracking in pavements.
Lamontagne, J., Dumas, P., Mouillet, V., Kistera, J., 2001. Comparison by Fourier transform infrared (FTIR) spectroscopy of different ageing techniques: application to road bitumens. Fuel 80, 483–488. https://doi.org/10.1016/S0016-2361(00)00121-6.
Li, J., Zhang, F., Liu, Y., Muhammad, Y., Su, Z., Meng, F., et al., 2019. Preparation and properties of soybean bio-asphalt/SBS modified petroleum asphalt. Construct. Build. Mater. 201, 268–277. https://doi.org/10.1016/j.conbuildmat.2018.12.206.
Li, L., Gao, Y., Zhang, Y., 2021. Fatigue cracking characterisations of waste-derived bitumen based on crack length. Int. J. Fatig. 142 https://doi.org/10.1016/j.ijfatigue.2020.105974.
Lu, X., Isacsson, U., 2001. Effect of binder rheology on the low-temperature cracking of asphalt mixtures. Road Mater. Pavement Des. 2 (1), 29–47. https://doi.org/10.1080/14680629.2001.9689893.
Lv, S., Peng, X., Liu, C., Qu, F., Zhu, X., Tian, W., et al., 2020. Aging resistance evaluation of asphalt modified by Buton-rock asphalt and bio-oil based on the rheological and microscopic characteristics. J. Clean. Prod. 257 https://doi.org/10.1016/j.jclepro.2020.120589.
Marateanu, M., Anderson, D., 1996. Time-temperature dependency of asphalt binders–An improved model (with discussion). J. Assoc. Asphalt Paving Technol. 65.
Marek, C.R., 1977. Low-temperature Properties of Bituminous Materials and Compacted Bituminous Paving Mixtures: A Symposium Presented at the Seventy-Ninth Annual Meeting, American Society for Testing and Materials. ASTM International, Chicago, Ill, p. 27. June-2 July 1976.
Mensching, D.J., Rowe, G.M., Daniel, J.S., Bennert, T., 2015. Exploring low-temperature performance in black space. Road Mater. Pavement Des. 16 (2), 230–253. https://doi.org/10.1080/14680629.2015.1077015.
Migliori, F., Corté, J.-F., 1998. Comparative study of RTFOT and PAV aging simulation laboratory tests. Transport. Res. Rec. 1638 (1), 56–63. https://doi.org/10.3141/1638-07.
Mohan, D., Pittman Jr., C.U., Steele, P.H., 2006. Pyrolysis of wood/biomass for bio-oil: a critical review. Energy Fuels 20 (3), 848–889. https://doi.org/10.1021/ef0502397.
MOTO, 2011. Standard test methods of bitumen and bituminous mixtures for highway engineering. In: JTG E20—2011.
MP19, A. S, 2010. Standard specification for performance-graded asphalt binder using multiple stress creep recovery (MSCR) test. In: American Association of State and Highway Transportation Officials: Washington, DC, USA.
Mullen, C.A., Boateng, A.A., 2008. Chemical composition of bio-oils produced by fast pyrolysis of two energy crops. Energy Fuels 22 (3), 2104–2109. https://doi.org/10.1021/ef700776w.
Nie, Y., Gao, W., Zhou, C., Yu, P., Song, X., 2020. Evaluation of ageing behaviors of asphalt binders using FTIR tests. Int. J. Pavement Res. Technol. 14 (5), 615–624. https://doi.org/10.1007/s42947-020-0210-1.
Olard, F., Di Benedetto, H., 2011. General "2S2P1D" model and relation between the linear viscoelastic behaviours of bituminous binders and mixes. Road Mater. Pavement Des. 4 (2), 185–224. https://doi.org/10.1080/14680629.2003.9689946.
Ouyang, C., Wang, S., Zhang, Y., Zhang, Y., 2006. Improving the aging resistance of asphalt by addition of Zinc dialkyldithiophosphate. Fuel 85 (7–8), 1060–1066. https://doi.org/10.1016/j.fuel.2005.08.023.
Petersen, J.C., 2009. A Review of the Fundamentals of Asphalt Oxidation: Chemical, Physicochemical, Physical Property, and Durability Relationships. Transportation Research Circular (E-C140).
Raouf, M.A., Williams, R.C., 2009. Determination of Pre-treatment Procedure Required for Developing Biobinders from Bio-Oils. Proceedings of the 2009 Mid-Continent Transportation Research Symposium,Ames, Iowa.
Raouf, M.A., Williams, R.C., 2011. Performance Properties of Fast Pyrolysis Bio-Oils Modified Asphalt. Paper presented at the 5th International Conference Bituminous Mixtures and Pavements, Greece.
Raouf, M.A., Metwally, M., Williams, R.C., 2010. Development of Non-petroleum Based Binders for Use in Flexible Pavements. IHRB Project TR-594, InTrans Project 08-133.
Rowe, G., 2011. Prepared Discussion Following the Anderson AAPT Paper Cited Previously. Paper presented at the AAPT.
Rowe, G.M., Baumgardner, G.L., Rossiter, W., Wallace, T., Dean, S.W., 2007. Evaluation of the rheological properties and master curve development for bituminous binders used in roofing. J. ASTM Int. (JAI) 4 (9). https://doi.org/10.1520/jai101016.
Ruan, Y., Davison, R.R., Glover, C.J., 2003. An investigation of asphalt durability: relationships between ductility and rheological properties for unmodified asphalts. Petrol. Sci. Technol. 21 (1–2), 231–254. https://doi.org/10.1081/lft-120016946.
Schwartz, S.E., 1993. Does fossil fuel combustion lead to global warming? Energy 18 (12), 1229–1248. https://doi.org/10.1016/0360-5442(93)90012-3.
Shan, L., Tian, S., He, H., Ren, N., 2017. Internal crack growth of asphalt binders during shear fatigue process. Fuel 189, 293–300. https://doi.org/10.1016/j.fuel.2016.10.094.
Shao, L., Wang, H., Zhang, R., Zheng, W., Hossiney, N., Wu, C., 2021. Analysis of the chemical properties and high-temperature rheological properties of MDI modified bio-asphalt. Construct. Build. Mater. 267, 121044 https://doi.org/10.1016/j.conbuildmat.2020.121044.
Stamatov, V., Honnery, D., Soria, J., 2006. Combustion properties of slow pyrolysis bio-oil produced from indigenous Australian species. Renew. Energy 31 (13), 2108–2121. https://doi.org/10.1016/j.renene.2005.10.004.
Sun, L., Wang, Y., Zhang, Y., 2014. Aging mechanism and effective recycling ratio of SBS modified asphalt. Construct. Build. Mater. 70, 26–35. https://doi.org/10.1016/j.conbuildmat.2014.07.064.
Sun, Z., Yi, J., Huang, Y., Feng, D., Guo, C., 2016. Properties of asphalt binder modified by bio-oil derived from waste cooking oil. Construct. Build. Mater. 102, 496–504. https://doi.org/10.1016/j.conbuildmat.2015.10.173.
Sun, Y., Wang, W., Chen, J., 2019. Investigating impacts of warm-mix asphalt technologies and high reclaimed asphalt pavement binder content on rutting and fatigue performance of asphalt binder through MSCR and LAS tests. J. Clean. Prod. 219, 879–893. https://doi.org/10.1016/j.jclepro.2019.02.131.
Tian, Y., Li, H., Zhang, H., Yang, B., Zuo, X., Wang, H., 2021. Comparative investigation on three laboratory testing methods for short-term aging of asphalt binder. Construct. Build. Mater. 266 https://doi.org/10.1016/j.conbuildmat.2020.121204.
Van den Bergh, W., 2011. The Effect of Ageing on the Fatigue and Healing Properties of Bituminous Mortars.

Wang, C., Castorena, C., Zhang, J., Kim, Y.R., 2015. Unified failure criterion for asphalt binder under cyclic fatigue loading. Road Mater. Pavement Des. 16 (2), 125–148. https://doi.org/10.1080/14680629.2015.1077010.

Wang, C., Zhang, H., Castorena, C., Zhang, J., Kim, Y.R., 2016. Identifying fatigue failure in asphalt binder time sweep tests. Construct. Build. Mater. 121, 535–546. https://doi.org/10.1016/j.conbuildmat.2016.06.020.

Wang, H., Ma, Z., Chen, X., Mohd Hasan, M.R., 2020. Preparation process of bio-oil and bio-asphalt, their performance, and the application of bio-asphalt: a comprehensive review. J. Traffic Transport. Eng. 7 (2), 137–151. https://doi.org/10.1016/j.jtte.2020.03.002.

Wang, R., Yue, M., Xiong, Y., Yue, J., 2021. Experimental study on mechanism, aging, rheology and fatigue performance of carbon nanomaterial/SBS-modified asphalt binders. Construct. Build. Mater. 268 https://doi.org/10.1016/j.conbuildmat.2020.121189.

Williams, M.L., Landel, R.F., Ferry, J.D., 1955. The temperature dependence of relaxation mechanisms in amorphous polymers and other glass-forming liquids. J. Am. Chem. Soc. 77 (14), 3701–3707.

Wu, S.-p., Pang, L., Mo, L.-t., Chen, Y.-c., Zhu, G.-j., 2009. Influence of aging on the evolution of structure, morphology and rheology of base and SBS modified bitumen. Construct. Build. Mater. 23 (2), 1005–1010. https://doi.org/10.1016/j.conbuildmat.2008.05.004.

Xiu, S., Shahbazi, A., 2012. Bio-oil production and upgrading research: a review. Renew. Sustain. Energy Rev. 16 (7), 4406–4414. https://doi.org/10.1016/j.rser.2012.04.028.

Xu, T., Huang, X., 2010. Study on combustion mechanism of asphalt binder by using TG–FTIR technique. Fuel 89 (9), 2185–2190. https://doi.org/10.1016/j.fuel.2010.01.012.

Yang, S.-H., Suciptan, T., 2016. Rheological behavior of Japanese cedar-based biobinder as partial replacement for bituminous binder. Construct. Build. Mater. 114, 127–133. https://doi.org/10.1016/j.conbuildmat.2016.03.100.

Yang, X., You, Z., 2015. High temperature performance evaluation of bio-oil modified asphalt binders using the DSR and MSCR tests. Construct. Build. Mater. 76, 380–387. https://doi.org/10.1016/j.conbuildmat.2014.11.063.

Yang, X., You, Z., Dai, Q., 2013. Performance evaluation of asphalt binder modified by bio-oil generated from waste wood resources. Int. J. Pavement Res. Technol. 6 (4), 431–439. https://doi.org/10.6135/ijprt.org.tw/2013.6(4).431.

Yang, X., You, Z., Dai, Q., Mills-Beale, J., 2014. Mechanical performance of asphalt mixtures modified by bio-oils derived from waste wood resources. Construct. Build. Mater. 51, 424–431. https://doi.org/10.1016/j.conbuildmat.2013.11.017.

Yang, X., You, Z., Mills-Beale, J., 2015. Asphalt binders blended with a high percentage of biobinders: aging mechanism using FTIR and rheology. J. Mater. Civ. Eng. 27 (4), 04014157 https://doi.org/10.1061/(ASCE)MT.1943-5533.0001117.

Yang, X., Mills-Beale, J., You, Z., 2017. Chemical characterization and oxidative aging of bio-asphalt and its compatibility with petroleum asphalt. J. Clean. Prod. 142, 1837–1847. https://doi.org/10.1016/j.jclepro.2016.11.100.

Yang, Y., Zhang, Y., Omairey, E., Cai, J., Gu, F., Bridgwater, A.V., 2018. Intermediate pyrolysis of organic fraction of municipal solid waste and rheological study of the pyrolysis oil for potential use as bio-bitumen. J. Clean. Prod. 187, 390–399. https://doi.org/10.1016/j.jclepro.2018.03.205.

You, Z., Mills-Beale, J., Fini, E., Goh, S.W., Colbert, B., 2011. Evaluation of low-temperature binder properties of warm-mix asphalt, extracted and recovered RAP and RAS, and bioasphalt. J. Mater. Civ. Eng. 23 (11), 1569–1574. https://doi.org/10.1061/(asce)mt.1943-5533.0000295.

Yusoff, N.I.M., Shaw, M.T., Airey, G.D., 2011. Modelling the linear viscoelastic rheological properties of bituminous binders. Construct. Build. Mater. 25 (5), 2171–2189. https://doi.org/10.1016/j.conbuildmat.2010.11.086.

Yusoff, N.I.M., Jakarni, F.M., Nguyen, V.H., Hainin, M.R., Airey, G.D., 2013. Modelling the rheological properties of bituminous binders using mathematical equations. Construct. Build. Mater. 40, 174–188. https://doi.org/10.1016/j.conbuildmat.2012.09.105.

Yut, I., Zofka, A., 2011. Attenuated total reflection (ATR) Fourier transform infrared (FT-IR) spectroscopy of oxidized polymer-modified bitumens. Appl. Spectrosc. 65 (7), 765–770. https://doi.org/10.1366/10-06217.

Zhang, Y., Gao, Y., 2019. Predicting crack growth in viscoelastic bitumen under a rotational shear fatigue load. Road Mater. Pavement Des. 22 (3), 603–622. https://doi.org/10.1080/14680629.2019.1635516.

Zhang, L., Xing, C., Gao, F., Li, T.-s., Tan, Y.-q., 2016. Using DSR and MSCR tests to characterize high temperature performance of different rubber modified asphalt. Construct. Build. Mater. 127, 466–474. https://doi.org/10.1016/j.conbuildmat.2016.10.010.

Zhang, R., Wang, H., You, Z., Jiang, X., Yang, X., 2017. Optimization of bio-asphalt using bio-oil and distilled water. J. Clean. Prod. 165, 281–289. https://doi.org/10.1016/j.jclepro.2017.07.154.

Zhang, R., Sias, J.E., Dave, E.V., 2020. Evaluation of the cracking and aging susceptibility of asphalt mixtures using viscoelastic properties and master curve parameters. J. Traffic Transport. Eng. https://doi.org/10.1016/j.jtte.2020.09.002.